2002 HST Calibration Workshop
Space Telescope Science Institute, 2002
S. Arribas, A. Koekemoer, and B. Whitmore, eds.

Statistical Analysis of ACS Data without Covariance in Errors

Kavan U. Ratnatunga

Carnegie Mellon University, Pittsburgh, PA 15213

Abstract. Careful statistical analysis is required to extract Cosmic Shear from ACS data. Rebinning the data to remove ACS image distortion creates images with adjacent pixels which have observational errors that are correlated. Proper statistical analysis of the image is complicated. It is however possible in principal to avoid any rebinning of the ACS data in the analysis of small galaxy images.

1. Introduction

In comparison to WFPC2 the distortion across the ACS image is 5 times larger. The pixel scale varies significantly so that full ACS images which are shifted by more than about an arcsecond cannot be stacked without correction for plate distortion. The relative image shift at CCD center translates to a different number of pixels close to the edge of the CCD. Most ACS dither patterns use a larger shift to close the gap between the CCD arrays.

The on-the-fly calibration (OTFC), designed to process full ACS images, rebins the data before stacking to identify cosmic rays. An iterative process is needed since rebinning before cosmic ray rejection bleeds the cosmic rays. The observational errors between adjacent pixels in resulting images have covariance complicating maximum likelihood or χ^2 image fitting which assumes independent errors in image pixels.

However, the typical faint galaxy images being surveyed with ACS in random pure parallel fields have half-light radius typically under a half arcsecond and the region used for image analysis is only about $6''$ square. Across this small region, the differential change in pixel scale from a region even $5''$ away in both directions, is small. In this case, at the edge of the $6''$ square region, the differential shift is about 0.2 pixels, with differential rotation of the two regions under 0.01 degrees (see Figure 2). For most of the higher signal-to-noise image pixels with greater weight in the analysis within the inner half arcsecond diameter region close to the center peaked galaxy image, it is more than a factor of 10 smaller. The changes in pixel scale and orientation within the region around the small galaxy image can therefore be ignored.

So to better than the accuracy used in the MDS WFPC2 analysis (cf. Figure 1), small individual galaxy images or stars from shifted ACS fields can be stacked and cosmic ray rejected without rebinning to correct for image distortion, even though the whole CCD image cannot be similarly stacked. Only the appropriate position dependent shifts corresponding to the shifts between images at the target reference pixel need to be computed using the adopted ACS distortion map. The small differential change in pixel scale is negligible for cosmic-ray rejection, which can now be redone without any image rebinning.

2. MDS-ACS Pipeline

The MDS-WFPC2 pipeline (Ratnatunga et al. 1999) software being modified for ACS will follow the following procedure.

1. Correct bias

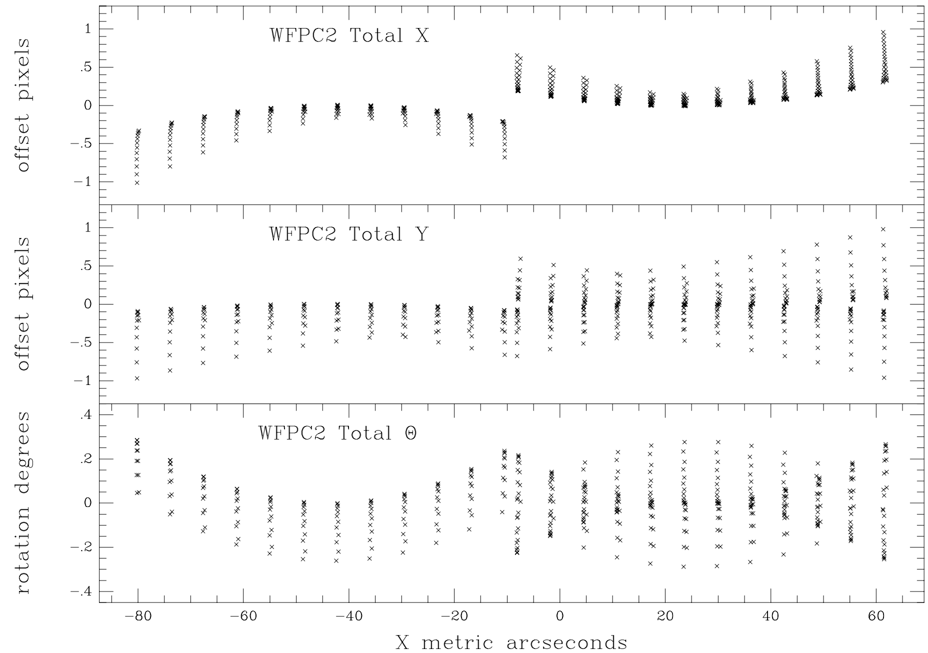

Figure 1. Total offset in X and Y and rotation at the corner of the $6''$ region used for image analysis relative to the center of each WFPC2 CCD array for a $5''$ shift in pointing in both X and Y. Most shifts used for MDS WFPC2 were a lot smaller than the extreme $7''$ used in this illustration.

2. Subtract dark current
3. Flag hot pixels
4. Flat field multiply by inverse sky flat and pixel area function, i.e., flux as expected for pixel-sky background less in smaller pixels.
5. Derive a rms error image along with calibrated image incorporating all sources of observational error.

Details of the calibrations adopted by MDS are discussed in Ratnatunga et al. (1995).

2.1. Shifts between Images

Initially, we adopt the IDT 4th order polynomial representation of ACS distortion mapping. This mapping is expected to line up images to about 0.1 pixels, and will be tested.

Shifts between images are determined by cross-correlation of the central region of the images. With ACS, if a larger region is needed to get a well defined peak, a rebinned ACS image would need to be used.

The image closest to the mean pointing is selected as the primary image to define the coordinate frame for the pure parallel fields in the sky.

2.2. Cosmic Ray Rejection

A minimum of 3 ACS exposures will be used in the stack. If images are all in a single line-of-sight, we stack calibrated not-rebinned ACS images. If not, we shift rebin the ACS images to a meta grid array of the primary image before stacking. This stacking is used to identify pixels hit by a cosmic ray in all individual images. The regions identified in each image as hit by a cosmic ray are used to flag pixels in the calibrated not-rebinned image. These ACS images are then shifted again and rebinned to a meta grid array without bleeding the pixels hit by cosmic rays and then stacked.

2.3. Object Identification

The cosmic ray clean stacked image is searched to identify all faint galaxy and stellar sources. The identified sources on this rebinned stack are used to identify a one-sigma contour around each object in the calibrated not-rebinned primary image. Using the relative shifts between the images and the ACS distortion map the centroid of the object can be located on each of the calibrated not-rebinned images.

We then compute the following using the adopted ACS distortion map at the location of the centroid of individual galaxy images.

- Pixel scale in X and Y directions
- Metapixel coordinates in arc-seconds from ACS reference pixel
- Orientation of X and Y with respect to PA_V3

Using equatorial coordinates of the ACS reference pixel and PA_V3 of pointing the estimated orientation of the galaxy in *observed* pixel coordinates can be converted directly to the standard frame of reference in the sky.

2.4. Image Analysis

A fixed size pixel array is cut out of each calibrated not-rebinned image for analysis, using the adopted ACS distortion map and the relative shifts between the images. Pre-computing the sub-pixel shifts between these individual images, the image analysis can now be done *without* stacking all of the exposures to a single image.

Assuming that the distortion is known better than the individual centers could be independently evaluated, it is better to use all of the images in the field to define the relative image shifts in position and orientation of the pointing, than let it be defined by only the images of galaxy being analyzed. As the relative shifts between the frames are predefined, it is not necessary to have extra parameters to define the centroid independently in each image of the galaxy.

The likelihood function is integrated over all of the observed ACS images with their individual error images in observed not-rebinned data space. The MDS analysis software creates a sub-pixelated centered galaxy model image, then after convolution shifts the image to the required pixel centroid. One could even convolve the galaxy model image independently based on the mean *HST* focus and pointing jitter during each exposure. The larger effect of jitter on parallel observations caused by differential aberration is discussed by Ratnatunga et al. (1997). All of the images required for integration of χ^2 over the pixels can be generated by shifting and block-binning the subpixelated image. The detector distortion caused by the non-orthogonal axes of ACS is included in this rebinning of the model image.

The same subpixelated convolved galaxy model image can be used if we ignore changes in focus and pointing jitter between exposures, and as long as there is no significant differential rotation.

By this approach we can overcome all of the limitations and possible errors of using the nearest integer shift in addition to the differences in telescope jitter and breathing of focus (consequently PSF) between exposures. This approach was discussed by Ratnatunga et al. (1994) in the *Image Restoration of HST Images* workshop ten years ago. It was not used by MDS for WF/PC and WFPC2 data to avoid the increase in computation time. The current generation of computers, which are 100 times faster than when the original MDS software was developed, may now make this approach practical.

However, the rms cumulative error caused by both the uncertainty in image ACS distortion maps, changes in telescope focus due to breathing and/or jitter in pointing, and differential pixel shifts over the image needs to be estimated. If that is larger than 0.3 pixels (15 mas), then to the known accuracy stacking cosmic ray rejected images using nearest integer shifts as done for MDS-WFPC2 may be the safest approach, including the additional 15 mas convolution in the image analysis.

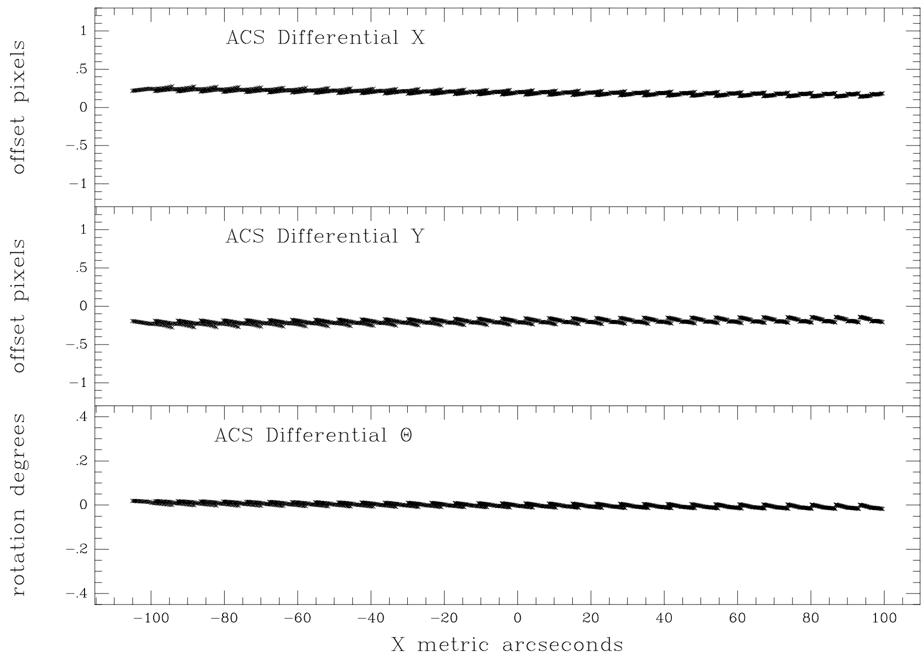

Figure 2. Differential offset in X and Y and rotation at the corner the of $6''$ region used for image analysis relative to the center of each galaxy image for a $5''$ shift in pointing in both X and Y. The vertical scale is the same as in Figure 1. Position dependent shifts for each image will be used for ACS stacking and analysis.

3. Conclusion

Calibrated but not rebinned ACS images can be used directly for analysis of small galaxy or stellar images, which then avoids using images with covariance. The same approach may also be useful for grism images.

Acknowledgments. I am grateful to Stefano Casertano who has always been a great help in discussing statistical issues of proper image analysis. This paper is based on observations with the NASA/ESA *Hubble Space Telescope*, obtained at the Space Telescope Science Institute. The *HST* research is funded by STScI grant GO9488.

References

Ratnatunga, K. U., Griffiths, R. E., & Casertano, S. 1994, in Proc. *The Restoration of HST Images and Spectra II*, eds. R. J. Hanish and R. L. White, p. 333

Ratnatunga, K. U., Griffiths, R. E., Neuschaefer, L. W., & Ostrander, E. J. 1995, in Proc. *HST Calibration Workshop II*, eds. A. Koratkar, A. & C. Leitherer, p. 351

Ratnatunga, K. U., Ostrander, E. J., & Griffiths, R. E. 1997, in Proc. *The 1997 HST Calibration Workshop*, eds. S. Casertano, et al., p. 361

Ratnatunga, K. U., Griffiths, R. E., & Ostrander, E. J. 1999, AJ, 118, 86